# Use of emanation thermal analysis to characterize microstructure development during Portland cement hydration

## V. Balek, J. Bydžovský, A. Dufka, R. Drochytka & I. N. Beckman

Springer

Springer

# Use of emanation thermal analysis to characterize microstructure development during Portland cement hydration

**V. Balek · J. Bydžovský · A. Dufka ·
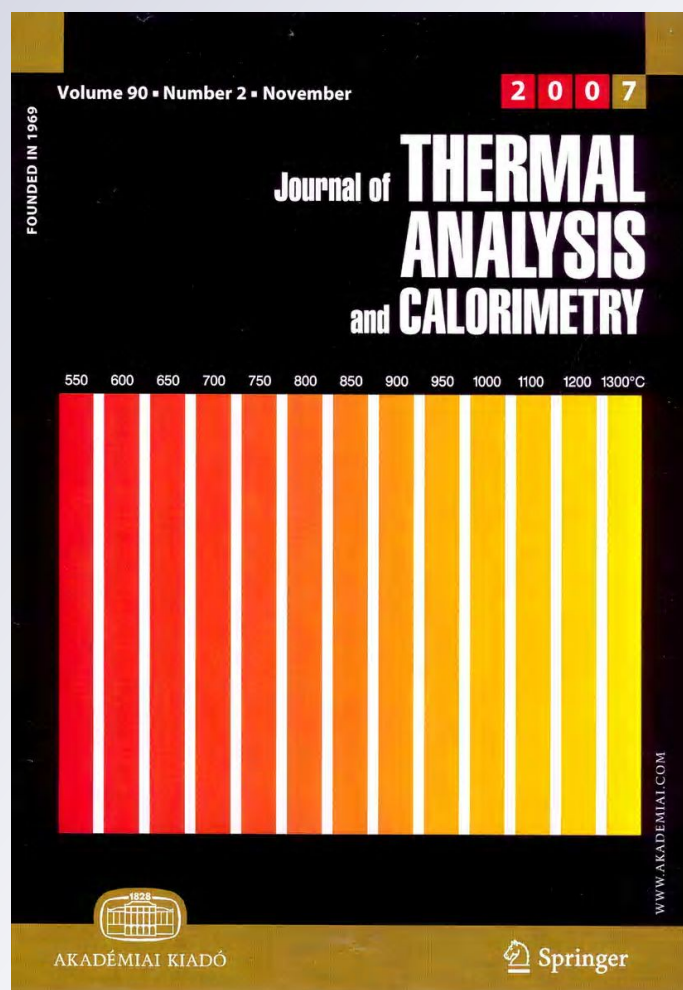R. Drochytka · I. N. Beckman**

**Abstract** Portland cement hydration has been investigated by emanation thermal analysis (ETA), based on the application of radon atoms as radioactive indicators. This method enabled us to characterize continuously changes in the microstructure of the cement paste at selected temperatures. The numerical simulation of time dependences of the emanating rate during cement hydration was carried out. An agreement between the mathematical model and experimental results of the ETA was obtained.

**Keywords** Emanation thermal analysis · Mathematical modeling · Microstructure changes · Portland cement

## Introduction

The hydration of Portland cement has been investigated by various methods, e.g., calorimetry, infrared spectroscopy, rheological measurement, electron microscopy, and others. These methods give various views of the course of the cement hydration process [1–3]. The emanation thermal analysis (ETA) [4, 5] based on the measurement of radon release from the previously labeled samples can be used to characterize the behavior of Portland cement samples during early hydration. The radon atoms do not react with the solid, in which they are incorporated in trace amounts before the measurement. The changes in the radon release rate reflect changes in the surface area and microstructure of the solid.

The objective of this article is to develop a numerical model for simulation of the radon release during the cement hydration and to compare it with the experimental results of the ETA characterizing microstructure changes during the cement hydration. The results will be applied in the technological study of the immobilization of nuclear waste by cementation.

## Experimental

### Materials

The Portland cement material (the PC-400 material of the surface area $0.3$ $m^2$ $g^{-1}$) was used for preparation of the cement paste samples by mixing with water in the water/cement ratio $w/c = 0.3$. The cement paste was homogenized by stirring.

At least 4 weeks before the preparation of the cement paste samples the Portland cement dry material was impregnated with acetone solution containing $^{228}Th$ and $^{224}Ra$ radioisotopes in the concentration of $10^3$ Bq per 1 ml, serving as a source of $^{220}Rn$ nuclides used in the ETA measurements [4–7]. The labeled dry samples were stored at 20 °C at least 4 weeks before the measurements to allow the radioactive equilibrium between the $^{228}Th$ and $^{224}Ra$ nuclides is established.

V. Balek (✉)
Nuclear Research Institute Řež, plc, 25068, Husinec-Řež,
Czech Republic
e-mail: bal@ujv.cz

J. Bydžovský · A. Dufka · R. Drochytka
Institute of Technology of Building Materials and Components,
Faculty of Civil Engineering, Brno University of Technology,
602 00, Brno, Czech Republic

I. N. Beckman
Chemical Faculty, Moscow State University, Moscow,
Russia 199234

Methods

*Emanation thermal analysis*

An equipment produced by NETZSCH Ltd., Selb, Germany in cooperation with the Nuclear Research Institute Řež, plc, Czech Republic was used for the ETA measurements.

The Portland cement paste sample in the amount of 1 g was measured being placed into a PVC vessel. During the ETA measurements the samples were kept at a constant temperature of 20, 35, and 45 °C. An air saturated with water vapor (relative humidity of 95 ± 3%) was used as a gas medium for the ETA measurements. The high relative humidity protected the sample from drying out during the experiment.

In the ETA measurements, the radon release rate $E$ is presented (in relative units) as $E = A_\alpha/A_{\text{total}}$, where $A_\alpha$ is $\alpha$ radioactivity of radon released in unit time from the labeled sample, and $A_{\text{total}}$ is the total $\gamma$ radioactivity of the labeled sample. The $A_{\text{total}}$ value is proportional to the rate of radon formation in the sample. Semiconductor and NaI(Tl) detectors were used for the $\alpha$ and $\gamma$ radioactivity measurements, respectively.

Radon atoms are formed as a result of spontaneous radioactive decay according to the scheme

$$^{228}\text{Th} \xrightarrow{\alpha} {}^{224}\text{Ra} \xrightarrow{\alpha} {}^{220}\text{Rn} \xrightarrow{\alpha}. \tag{1}$$
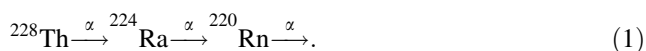
By using $^{228}$Th (half life 1.9 years) as the parent radionuclide, a practically permanent source of $^{220}$Rn (half life 55.8 s) is incorporated into the sample.

The cement sample was labeled by impregnation with an acetone solution containing $^{228}$Th and $^{224}$Ra in the concentration of the order of $10^5 \text{ s}^{-1} \text{ cm}^{-3}$. During the labeling the radionuclides are adsorbed on the surface of the cement grains. The specific activity of the samples labeled is $10^3$–$10^4 \text{ s}^{-1} \text{ g}^{-1}$ of sample. The atoms of $^{224}$Ra and $^{220}$Rn are incorporated into the cement grains to a maximum depth of 120 nm as a consequence of the recoil energy 85 keV/atom which every atom gains during the decay of its parent nuclides [5].

The radon release rate called emanation rate, $E$, can be expressed by Eq. 2:

$$E = S_{\text{eff}} \left[ K_1 + K_2 \left( \frac{D_i}{\lambda} \right)^{1/2} \right] \cdot \rho, \tag{2}$$

where $S_{\text{eff}}$ is the effective surface area related to the mass of the sample, $K_1$, $K_2$ are constants, $D$ is the radon diffusion coefficient in the solid, $\rho$ is the density, and $\lambda$ is the $^{220}$Rn radon decay constant ($\lambda = 0.0127 \text{ s}^{-1}$).

Penetration resistance, $R_F$, was determined as the ratio of the strength needed for the penetration of a cylindrical indentor of an 1 mm$^2$ into a sample of the setting cement paste to the depth of 5 mm, to the cross-sectional area. Then standard Vicat test was used for checking the beginning and end of the setting period of the cement paste.

## Results

Computer modeling of radon release during Portland cement hydration

In the evolution of the structure of hardened cement paste several stages are usually distinguished:

(a) the period of initial hydration, occurring immediately after the mixing of cement with water; resulting hydration products formed a layer on the surface of cement which stops the hydration reaction;

(b) the induction period, taking place after the formation of hydration products on the surface of the cement grains. The structure of the cement paste has a coagulated character and the rate of hydration reactions is low;

(c) the period of the destruction of the formed layer by the hydration products, during which the rate of the hydration reaction substantially increases;

(d) the period of the gradual slowing down of the hydration reactions. In this period, the hydration is limited by the diffusion of water through the hydration product layer.

The evolution of the structure of the hardened cement paste is controlled by a number of physico-chemical processes, in the course of which the initial coagulation structure of the cement paste changes into the thermodynamically more stable structure of the cement stone. In this article, the curves obtained by the ETA are discussed with regard to the stages of the hydration process mentioned above.

## A model of cement hydration supposing the formation of an intermediate metastable phase

In the modeling, we have considered the formation of intermediate metastable hydration products, which are transformed into final hydration products.

Following parameters were used in the modeling radon release rate: $L$—the thickness of sample, $E$—emanation rate of the sample, $D_1$, $D_2$, and $D_3$—the radon diffusion coefficients in the initial, final, and intermediate solid state phases denoted by numbers 1, 2, and 3, respectively ($D_3 \gg D_1$ and $D_3 \gg D_2$).

In the frame of the parallel diffusion mechanisms, we have supposed that the total value of the emanation rate of the sample is composed by the sum of the emanation rate values of individual phases 1, 2, and 3.

In the conditions of the isothermal solid state reaction we can write

$$E(t) = E_1\alpha_1(t) + E_2\alpha_2(t) + E_3\alpha_3(t), \tag{3}$$

where the volume fractions $\alpha_1$, $\alpha_2$, and $\alpha_3$ of the phases are ($\alpha_1 + \alpha_2 + \alpha_3 = 1$).

The emanation rate of the slab-like sample can be expressed as follows:

$$E_i = \frac{1}{L}\left(\frac{D_i}{\lambda}\right)^{1/2} thL\left(\frac{\lambda}{D_i}\right)^{1/2}, \tag{4}$$

where $\lambda$ is the radioactive decay constant of radon, $D_i$ is the radon diffusion coefficient in an individual phase $i$ of the solid sample.

The temperature dependence of the radon diffusion coefficient, $D$, can be written as follows, considering Arrhenius law

$$D = D_0 \exp\left(-\frac{Q}{RT}\right), \tag{5}$$

where $Q$ is the activation energy of radon diffusion in the respective solid phase, $D_0$ is the pre-exponential factor characterizing the respective lattice property, and $T$ is the temperature in Kelvin.

During the random nucleation the time dependence of the decrease of the amount of the phase 2 is determined by the integral Gauss distribution curve

$$\alpha_2(t) = \mathrm{erf}z = \frac{2}{\pi^{1/2}}\int_0^z \exp\left(-t^2\right)dt, \tag{6}$$

where the increase in the amount of the phase 2 can be written as

$$\alpha_1(t) = 1 - \alpha_2(t) = \mathrm{erfc}z = 1 - \mathrm{erf}z. \tag{7}$$

The time dependence of the phase 3 amount is expressed by the differential Gauss distribution curve

$$\alpha_3(t) = A\frac{d[\alpha_2(Kt - \tau_0)]}{dt}, \tag{8}$$

where $A$ is the amount of elemental crystallographic cells of the intermediate phase 3, which are formed after the disappearance of the elemental cell of the initial phase 1. This parameter determines the height of the curve corresponding to the function $\alpha_3(t)$; $K$ is the equilibrium constant of the chemical reaction underlying the formation of the intermediate phase 3, it can be expressed as the ratio $K = k_{form}/k_{transform}$, where $k_{form}$ is the rate constant of the intermediate phase 3 formation, $k_{transform}$ is the rate

constant of its transformation into the final phase 2. The equilibrium constant $K$ determines the height of the function, representing $\alpha_3(t)$, which reflects the intensity of the solid state transformation; $\tau_0$ is the parameter determining the position of the $\alpha_3(t)$ function of the time axis.

The calculations made by Eqs. 6–8 enabled us to obtain time dependences of the concentrations of the initial, final, and intermediate phases, respectively. As it follows from Fig. 1, the amount of the initial phase monotonously decreased from 1 to 0 (curve 1) whereas the amount of the final phase increased from 0 to 1 (curve 2). The time dependence of the amount of the intermediate metastable phase 3 is described by a peak-like curve (curve 3). Using Eq. 3 and taking into account Eqs. 4–6 a peak-like ETA curve resulted from the model (Fig. 1, curve 4). In the ETA curve modeling, we have supposed that the solid sample was labeled by the radionuclides of $^{228}$Th and $^{224}$Ra representing a quasi-permanent source of radon $^{220}$Rn atoms.

Following parameters characterizing the radon mobility, i.e., microstructure permeability and surface area during the hydration process were considered: $E_1 = 0.02$, $E_2 = 1$, $E_3 = 0.2$. It means that the value $E_3$ of the intermediate metastable phase was 50 times higher than the $E_1$ value corresponding to the initial phase, and 5 times higher than the value $E_2$ corresponding to the final reaction product. The calculations were carried out considering the following parameters of the hydration reaction: $A = 0.25$, $K = \tau_0 = 2.2$. The isothermal conditions of the thermal decomposition were considered. These parameters correspond to the real experiment, as the intermediate phase possesses much higher disorder degree than the initial and final phases.
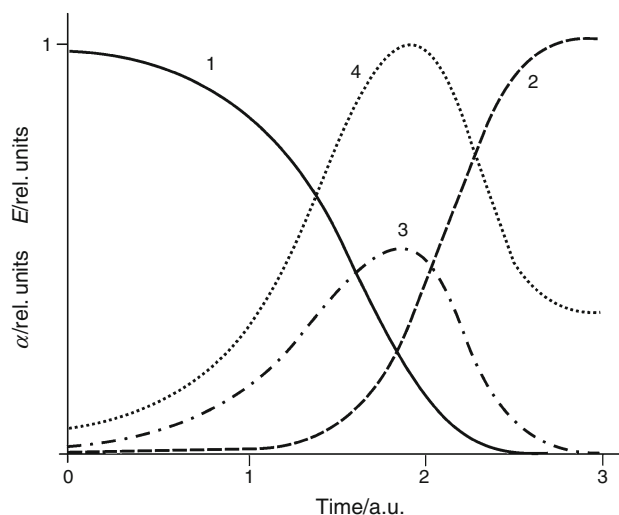


**Fig. 1** Time dependences of the concentrations of individual phases: initial (curve 1), final phase (curves 2) and intermediate phase (curve 3), and ETA curve (curve 4) resulting from the computer model
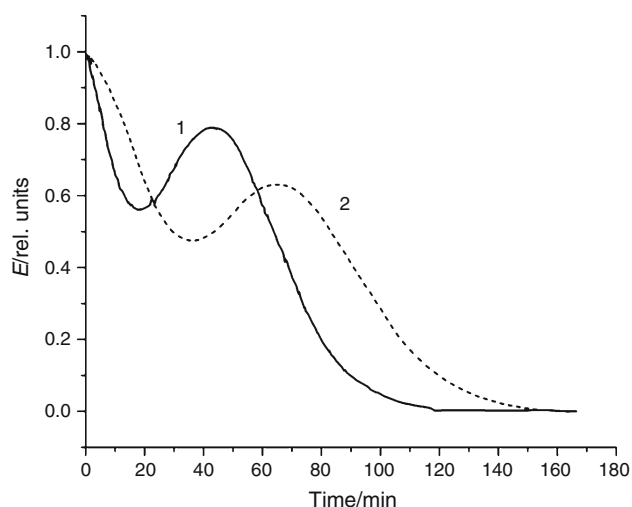
**Fig. 2** Results of the computer modeling of the effect of hydration temperature on the time dependence of the emanation rate, $E$, in the initial period of the cement hydration. Curves 1 and 2 correspond to the hydration processes at temperatures of 35 and 45 °C, respectively



**Fig. 3** Comparison of the experimental results of ETA (curve 1), the penetration resistance $R_F$ (curve 2), and the results of the Vicat test measured at the temperature of 20 °C; the water to cement ratio $w/c = 0.3$

Using this model [6] for simulating time dependences of the radon release rate during the hydration process reaction, it was demonstrated that the radon mobility measurements can characterize the changes in the microstructure of the sample of hydraulic binders.

This approach enabled us to consider different morphology for the reaction intermediate products with regard to the initial solid sample and final reaction products.

When using this model in the numerical simulation of time dependence of the radon release rate, $E$, following behavior and properties of the hydrated cement paste were considered during the early hydration stage.

(i)   Decrease of the surface area of the sample when cement paste is formed (curve 1, Fig. 1)
(ii)  Increase of emanation rate due to formation of the gel-like hydration products in the cement paste (Curve 3, Fig. 1)
(iii) Decrease of the surface area due to crystallization of the gel-like products in the cement paste resulting in the setting and hardening of the sample.

From Fig. 2, it is obvious that due to the temperature increase of the cement hydration from 35 to 45 °C a shift of the time interval of setting took place. The subsequent decrease of the emanation rate, $E$, corresponding to the setting and hardening of the hydrated cement paste, was shifted to the lower times from the onset of the hydration.

## Experimental results

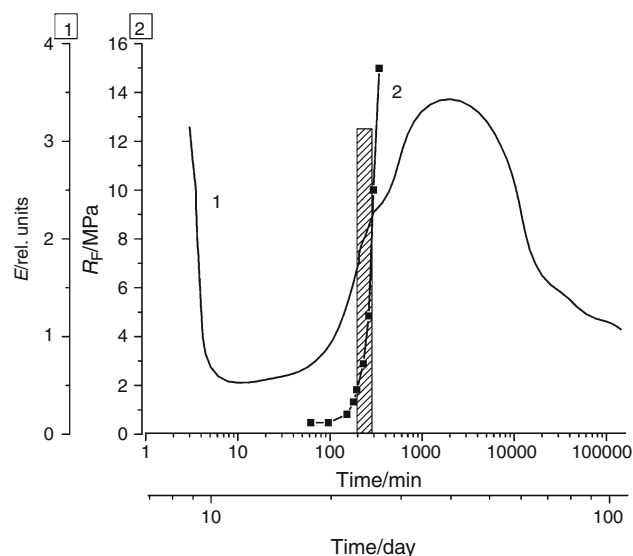In Fig. 3, the results of ETA (curve 1) are presented together with results of the measurement of the penetration resistance (curve 2) measured during hydration of the cement paste at the temperature of 20 °C.

It is obvious from Fig. 3 that the changes in the radon release rate (ETA results) indicated the difference in the behavior of the sample, namely: the initial hydration period which takes place immediately after mixing the cement with water, the induction period, the accelerated period, and the final hydration period. On mixing the cement with water, the radon release rate, $E$, rapidly increased, indicating the first interaction of the surface of the cement grains with water, whereas after several minutes the observed decrease of the radon release rate, $E$, indicated the formation of the layer of the hydration products, which resulted in slowing down of the rate of the initial hydration. The layer possesses low permeability not only for the water molecules but also for the radon atoms released from the labeled cement paste sample and indicated the structure changes of the cement paste. The induction period is characterized by a relatively low values of the radon release rate, $E$, indicating that the hydration is practically stopped. The reactivation of the hydration process caused by the penetration of water into the not reacted cement grains is characterized by an increase of the radon release rate, $E$. The values of $E$ are assumed to be proportional to the hydration rate. In course of the hydration process the products of the hydration limit the radon release rate from the sample. At the end of the induction (dormant) period the increase of the radon release rate, $E$, was observed.

The subsequent changes in the decrease of the radon release rate are due to microstructure changes during setting and hardening of the cement paste. It can be mentioned

that the use of ETA makes it possible to determine the time interval of the cement hydration more precisely than the traditional methods commonly used, e.g., the penetration resistance.

The onset of the radon release rate, $E$, increases (see curve 1, Fig. 3), which indicates the end of the induction period takes place earlier than the observed changes of the penetration resistance (see curve 2, Fig. 3.) This is due to the principles of the respective methods. The ETA results indicated the changes taking place in the in the labeled surface layer of the cement grain, whereas the penetration resistance reflects changes in the mechanical properties of the bulk of the hydrating sample tested. It is evident that the increase the penetration resistance (curve 2) fits well with the inflection of the radon release rate, $E$, observed on the ETA curve (curve 1). Its follows from the experimental ETA results, presented as curve 1, Fig. 3, that the numerical model developed (see Fig. 1) is in a good agreement with the experimental testing by means of the ETA.

It was shown that the ETA can be used in the investigation of Portland cement hydration at various temperatures.

Figure 4 depicts the ETA results obtained by investigating the Portland cement during hydration at the different temperatures of 35 °C (curve 2) and 45 °C (curve 1).

The ETA results of the cement hydration at the various temperatures presented in Fig. 4 can be used to characterize the differences the microstructure development during the cement setting, as accelerated at the elevated temperatures.

The use of the ETA gives the possibility to characterize the effect of the respective technological temperature conditions. The advantage of this method consists in the possibility of investigating the evolution of the hardened cement paste structure continuously. The results obtained by ETA can be used also for the evaluation of various cement types from the viewpoint of temperature influence on their hydration.

A good agreement between the results of numerical simulation and experimental results of the ETA was found.

## Conclusions

It was demonstrated that the ETA makes it possible to characterize the early stages of the cement paste setting. The ETA offers new insights into the development of the microstructure during cement hydration. This method can be applied to the investigation of the secondary changes in the cement hydration products as well as to characterize the effect of temperature on the microstructure development.

A good agreement between the results of numerical simulation and experimental ETA results was found. The proposed numerical model can be used in the microstructure diagnostics of the cement hydration. The ETA method can be applied to characterize the fixation of radioactive waste by cementation, where the temperature used for the cementation may affect the chemical durability of the hardened cement paste in the radioactive waste repository conditions.

**Fig. 4** Time dependences of the radon release rate, $E$, measured during the Portland cement hydration at the temperature of 35 °C (curve 2) and 45 °C (curve 1). The ratio of water to cement was $w/c = 0.3$

## References

1. Bhatty JI. A review of the application of thermal-analysis to cement admixture systems. Thermochim Acta. 1991;189:313–50.
2. Ylmen R, Jalgid U, Steenari BM, Panas I. Early hydration and setting of Portland cement monitored by IR, SEM and Vicat techniques. Cem Concr Res. 2009;41:433–9.
3. Scrivener KL, Nonat A. Hydration of cementitious materials, present and future. Cem Concr Res. 2011;41:651–65.
4. Balek V, Tölgyessy J. Emanation thermal analysis and other radiometric emanation methods. In: Svehla G, editor. Comprehensive analytical chemistry Part XIIC. Amsterdam: Elsevier; 1984.
5. Balek V, Šubrt J, Mitsuhashi T, Beckman IN, Györyová K. Emanation thermal analysis ready to fulfill the future needs of materials characterization. J Therm Anal Calorim. 2002;67:15–35.
6. Balek V, Beckman IN. Theory of emanation thermal analysis X. Characterization of morphology changes during hydration of cementitious binders. J Therm Anal Calorim. 2002;67:37–47.
7. Tatlisu H, Balek V, Beckman IN, Kardjilov N, Hilger A, Rauch H. Imaging and diffusion structural diagnostics of silicon carbide-based composites and fibers. J The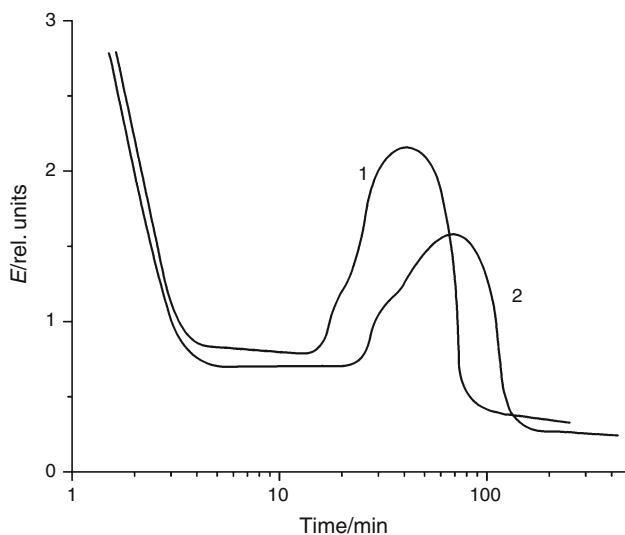rm Anal Calorim. 2012;107:447–52.